

28. R. M. Cooke *et al.*, *Nature* **327**, 339 (1987).
 29. K. Kurachi and E. W. Davie, *Proc. Natl. Acad. Sci. U.S.A.* **79**, 6461 (1982).
 30. K. B. M. Reid *et al.*, *Immunol. Today* **7**, 230 (1986).
 31. A. Nicholson-Weller, J. Zaia, M. G. Raum, J. E. Coligan, *Immunol. Lett.* **14**, 307 (1986-1987).
 32. L. B. Klickstein *et al.*, *J. Exp. Med.* **165**, 1095 (1987).
 33. M. Carroll *et al.*, *ibid.* **167**, 1271 (1988).
 34. W. M. Gallatin, I. L. Weissman, E. C. Butcher, *Nature* **304**, 30 (1983); M. Siegelman *et al.*, *Science* **231**, 823 (1986).
 35. R. P. McEver and M. N. Martin, *J. Biol. Chem.* **259**, 9799 (1984); P. E. Stenberg, R. P. McEver, M. A. Shuman, Y. V. Jacques, D. F. Bainton, *J. Cell Biol.* **101**, 880 (1985); S.-C. Hsu-Lin, C. L. Berman, B. C. Furie, D. August, B. Furie, *J. Biol. Chem.* **259**, 9121 (1984); G. I. Johnston, A. Kurosky, R. P. McEver, *ibid.*, in press.
 36. L. Lasky *et al.*, *Cell*, in press.
 37. G. I. Johnston, R. G. Cook, R. P. McEver, *ibid.*, in press.
 38. A. F. Williams and A. N. Barclay, *Annu. Rev. Immunol.* **6**, 381 (1988); L. Hood, M. Kronenberg, T. Hunkapiller, *Cell* **40**, 225 (1985).
 39. D. Simmons, M. W. Makgoba, B. Seed, *Nature* **331**, 624 (1988); D. E. Staunton, S. D. Marlin, C. Stratowa, M. L. Dustin, T. A. Springer, *Cell* **52**, 925 (1988).
 40. R. O. Hynes, *Cell* **48**, 549 (1987); T. K. Kishimoto, K. O'Connor, A. Lee, T. M. Roberts, T. A. Springer, *ibid.*, p. 681.
 41. E. Ruoslahti and M. D. Pierschbacher, *Science* **238**, 491 (1987).
 42. D. M. Lewisohn, R. F. Bargatze, E. C. Butcher, *J. Immunol.* **138**, 4313 (1987).
 43. T. A. Yednock, L. M. Stoolman, S. D. Rosen, *J. Cell Biol.* **104**, 713 (1987); T. A. Yednock, E. C. Butcher, L. M. Stoolman, S. D. Rosen, *ibid.*, p. 725.
 44. M. E. Wheeler, F. W. Lusinskas, M. P. Bevilacqua, M. A. Gimbrone, Jr., *J. Clin. Invest.* **82**, 1211 (1988).
 45. M. P. Bevilacqua and M. A. Gimbrone, Jr., unpublished observation.
 46. G. W. Smith *et al.*, *J. Clin. Invest.* **82**, 1746 (1988).
 47. M. L. Dustin, R. Rothlein, A. K. Bhan, C. A. Dinarello, T. A. Springer, *J. Immunol.* **137**, 245 (1986).
 48. M. Patarroyo, E. A. Clark, J. Prieto, C. Kantor, C. G. Gahmberg, *FEBS Lett.* **210**, 127 (1987).
 49. J. S. Pober *et al.*, *J. Immunol.* **137**, 1893 (1986).
 50. P. R. Streeter, E. L. Berg, B. T. N. Rouse, R. F. Bargatze, E. C. Butcher, *Nature* **331**, 41 (1988).
 51. P. R. Streeter, B. T. N. Rouse, E. C. Butcher, *J. Cell Biol.* **107**, 1853 (1988).
 52. P. J. Simpson *et al.*, *J. Clin. Invest.* **81**, 624 (1988).
 53. N. B. Vedder *et al.*, *ibid.*, p. 939.
 54. We thank the members of our laboratories for helpful discussions, T. Collins and R. Cotran for critical review of the manuscript, L. Lasky for providing the unpublished sequence of the mouse lymphocyte homing receptor, R. McEver and G. Johnston for sharing their unpublished data on GMP-140, and J. Kim for technical assistance. Supported by NIH grant PO1 HL-36028 and by a grant from Hoechst AG.
 22 December 1988; accepted 30 January 1989

Mouse Lymph Node Homing Receptor cDNA Clone Encodes a Glycoprotein Revealing Tandem Interaction Domains

MARK H. SIEGELMAN, MATTHIJS VAN DE RIJN, IRVING L. WEISSMAN

Isolation of a clone encoding the mouse lymph node homing receptor reveals a deduced protein with an unusual protein mosaic architecture, containing a separate carbohydrate-binding (lectin) domain, an epidermal growth factor-like (EGF) domain, and an extracellular precisely duplicated repeat unit, which preserves the motif seen in the homologous repeat structure of complement regulatory proteins and other proteins. The receptor molecule is potentially highly glycosylated, and contains an apparent transmembrane region. Analysis of messenger RNA transcripts reveals a predominantly lymphoid distribution in direct relation to the cell surface expression of the MEL-14 determinant, and the cDNA clone is shown to confer the MEL-14 epitope in heterologous cells. The many novel features, including ubiquitination, embodied in this single receptor molecule form the basis for numerous approaches to the study of cell-cell interactions.

A FUNDAMENTAL EVENT REQUIRED FOR THE DEVELOPMENT of lymphoid organs and for appropriate progression of the immune response resides at the interface between a lymphocyte's mobile circulating phase and its relatively sessile phase within a particular lymphoid organ. The specific portal of entry of lymphocytes from bloodstream into peripheral lymphoid organs was identified as specialized postcapillary venules bearing unusually high-

walled endothelia (1-3), and named high endothelial venules (HEV's) (4). The fundamental role of HEV-lymphocyte interaction in lymphocyte trafficking has been demonstrated (5, 6). Recirculating lymphocytes, but not other blood-borne cells, specifically recognize and adhere to luminal walls, and migrate through this highly specialized endothelium into the lymphoid organ parenchyma. Both B and T lymphocytes enter lymphoid organs via common HEV's (5-8), and thereafter migrate to T cell or B cell domains (9-11). Recirculation of lymphocytes from bloodstream to particular sites has been called "homing," and the cell surface structures mediating recognition and adherence to lymphoid organ HEV's have been called "homing receptors" (12).

Migration of lymphocytes from blood to lymphoid organs occurs nonrandomly. Peripheral node lymphocytes exhibit binding preference for peripheral node HEV's, while binding to Peyer's patch HEV is favored by lymphocytes derived from Peyer's patches (13). Specificity of homing results from the particular array of homing receptors actively expressed by any one lymphocyte (9, 14, 15). Subsequent studies of lymphocyte populations and cell lines showed mutually exclusive homing to either lymph node HEV or Peyer's patch HEV, an indication that the two specificities are mediated by independent cell surface structures. A significant proportion of murine lymphomas are unispecific with regard to Peyer's patch or peripheral lymph node HEV binding (12), while others recognize neither venule type. Therefore, lymphocyte homing appears to be

The authors are in the Laboratory of Experimental Oncology, Department of Pathology, Stanford University School of Medicine, Stanford, CA 94305.

Fig. 1. Amino-terminal protein sequence analysis of gp90^{MEL-14}. The NH₂-terminal protein sequence obtained by auto-

	5	10	15	20	25	30	35																														
W	T	Y	H	Y	-	-	K	P	M	-	W	-	-	-	K	F	-	K	-	-	Y	-	-	V	(V)	I	-	-	K	-	-	-	(Y)				
W	T	Y	H	Y	S	E	K	P	M	N	W	E	N	-	A	R	K	F	C	K	Q	N	Y	T	D	L	V	A	I	Q	N	K	R	E	I	E	Y
TGG	ACT	TAC	CAT	TAT	TCT	GAA	AAA	CCC	ATG	AAC	TGG	GAA	AAT	-	GCT	AGA	AAG	TTC	TGC	AAG	CAA	AAT	TAC	ACA	GAT	TTA	GTC	GCC	ATA	CAA	AAC	AAG	AGA	GAA	ATT	GAG	TAT

matized sequence analysis of material purified from extracts of cells reacting with MEL-14 is compared to the protein sequence encoded by the mLHR_c cDNA clone. The nucleotides 169 to 279 are shown with the predicted amino acids above. The top line shows the sequence obtained by ³H- and ³⁵S-labeled sequence analysis (24). Definite determinations are indicated by the appropriate residue; tentative determinations are indicated by the residue in parentheses. Dashes indicate positions where no amino acid determination could be made by this method. Purification of gp90^{MEL-14} from EL-4-MEL-14hi cells metabolically labeled with isotopically labeled amino acids was performed (24) with the use of the monoclonal antibody MEL-14. Automated sequence analysis (Applied Biosystems Model 470A) (61) was modified to bypass the flask for conversion of thiazolinone derivatives (24). Entire butyl chloride extracts containing the 2-anilino-thiazolinone derivatives at each step were transferred to vials directly for scintillation counting.

Positions containing radioactivity above background indicated the presence of a particular ³H- or ³⁵S-labeled amino acid. A 32-fold degenerate 15-base oligonucleotide corresponding to the NH₂-terminal five amino acids of the mature protein, Trp-Thr-Tyr-His-Tyr, was designed. Synthesis was performed in four pools containing eight-fold degeneracy each, corresponding to the following sequences: (i) 5' TGG AC(T/C) TA(T/C) CA(T/C) TAT 3'; (ii) 5' TGG AC(T/C) TA(T/C) CA(T/C) TAC 3'; (iii) 5' TGG AC(A/G) TA(T/C) CA(T/C) TAT 3'; (iv) 5' TGG AC(A/G) TA(T/C) CA(T/C) TAC 3'. Oligonucleotide probes were synthesized by the phosphoramidite method (62) (Applied Biosystems 380A DNA synthesizer) and purified on acrylamide gels (63). The probes corresponded to the mRNA coding (sense) strand. Similar probes corresponding to the opposite (anti-sense) strand were also synthesized and used. Oligonucleotides were labeled with [γ -³²P]ATP and T₄ polynucleotide kinase to 2 × 10⁸ dpm/μg (64).

regulated by the expression of complementary adhesion molecules on each of the two participants, the homing receptors on recirculating lymphocytes, and the vascular "addressins" on specialized particular organ HEV's (12, 16), thereby influencing distribution of lymphocytes within an organism.

The availability of clonal lymphoid cell lines with exclusive specificity for a single HEV type presented the opportunity to define directly the cell surface structures involved in the HEV recognition process. A monoclonal antibody, MEL-14, was developed that detects a cell surface determinant present only on those murine T and B cells that bind peripheral lymph node HEV's, but not on those which bind either Peyer's patch HEV only or have no HEV binding activity at all (12). In addition, MEL-14 specifically ablates binding of normal or neoplastic cells to peripheral node HEV's, and selection of clonal variants with altered expression of the MEL-14 determinant precisely parallels adherence activity to HEV's on in vitro assay. The presence of homing receptors on neoplastic lymphoid cells provides an accurate indication of the lymphoid organs to which they metastasize (17, 18). The concordance of these observations suggests that the monoclonal antibody recognizes the actual receptor. Cell surface structures implicated in HEV binding have also been identified in other species (19-23).

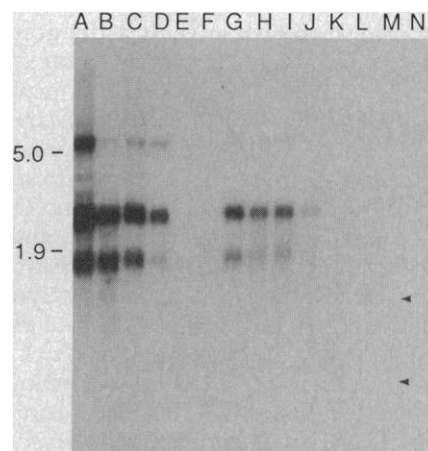
MEL-14 specifically precipitates from the cell surface of lymph node HEV-binding lymphocytes a protein species with apparent molecular size of about 90 kD (12), which we have designated gp90^{MEL-14} (24). Partial sequence analysis of the amino terminus of this molecule purified to homogeneity revealed the presence of two amino termini, one corresponding to the amino terminus of the highly conserved polypeptide ubiquitin, and the other to a sequence representing the core polypeptide of the receptor (24). These findings, in concert with λ gt11 screening and epitope mapping studies (25), lead to a proposed model of the receptor complex as a core polypeptide modified by ubiquitination and extensive glycosylation. In addition, it was inferred from functional correlates that the region of the site (or sites) of ubiquitination might participate in the adhesion event. In order to characterize the mouse lymph node homing receptor, and therefore its relation to other known cell-cell, cell-substrate, and other heterotypic protein interactions, we cloned the cDNA that encodes the core peptide of the mouse lymph node homing receptor, hereafter designated mLHR_c.

We now describe (i) our amino acid sequence analysis of the core polypeptide, from which we obtained an oligonucleotide probe, and (ii) the isolation and characterization of a cDNA clone encoding the core polypeptide of gp90^{MEL-14}. The distribution of expression of the hybridizing transcripts appears to be restricted to lymphoid cells and tissues, and transfection into heterologous cells confirms expression of the MEL-14 epitope. Examination of the mLHR_c cDNA

clone sequence reveals a potentially highly glycosylated transmembrane protein with a short cytoplasmic tail. Unusual features inherent in the sequence include an extracytoplasmic tandem array of protein domains.

Oligonucleotide approach to isolation of mLHR_c. EL4-MEL-14hi cells were metabolically labeled with all essential tritiated amino acids, one amino acid per experiment, and affinity and gel-purified material was subjected to automated NH₂-terminal Edman degradation (24). The results of this analysis for the major (nonubiquitin) sequence representing the putative core polypeptide is shown in Fig. 1. Some of these assignments have been described (24). Unambiguous amino acid assignments could be made at 16 of the NH₂-terminal 32 residues, and an additional tentative tyrosine position was made at residue 37. Whereas earlier analysis gave some evidence for a leucine at position 31, subsequent repetition did not confirm any leucine assignments in NH₂-terminal sequencing runs. The tentative assignment at position 28 was due to the inability to distinguish between an actual valine versus incomplete cleavage and partial loss of phase from the valine in the previous position 27.

Fig. 2. mRNA blot hybridization analysis of MEL-14 positive and negative tissues and cell lines. The index cell line in these studies was EL-4-MEL-14hi, a variant of the continuous T cell lymphoma cell line, EL-4, selected by fluorescence activated flow cytometry for high level expression of the MEL-14 antigen, a property that cosegregated with the capacity to bind peripheral node venules. Additional variants of EL-4, differing with respect to gp90^{MEL-14}



expression were obtained from various sources, after fluorescence activated cell sorter (FACS) analysis. Both C6V1 and VL3 are radiation-induced leukemia virus thymoma clonal cell lines. RNA blot analysis was performed by the formaldehyde procedure (65), on a variety of poly(A)-selected RNA species isolated from various tissues and cell lines. Approximately 5 μg of RNA were applied to each gel lane. Hybridization was to full-length probe labeled with [³²P]dCTP by the random primer procedure (66). (Lane A) EL-4-MEL-14xhi; (lane B) EL-4-MEL-14hi; (lane C) BD EL-4-MEL-14hi; (lane D) EL-4-MEL-14lo; (lane E) BD EL-4-MEL-14neg; (lane F) C6V1; (lane G) VL-3; (lane H) thymus; (lane I) spleen; (lane J) mesenteric lymph node; (lane K) liver; (lane L) kidney; (lane M) testes; (lane N) brain. Arrows indicate position of transcripts in testes.

Among nonessential amino acids only proline rendered an unambiguous position call.

Screening of approximately 7.5×10^5 λ ZAP (Stratagene) plaques of an EL4-MEL-14hi cDNA library (26) with degenerate synthetic oligonucleotides corresponding to the NH₂-terminal five amino acids resulted in the identification of 58 independent isolates. After the plaques were purified, each contained a single insert, with sizes ranging from 700 to 3000 base pairs and which consistently hybridized with the oligonucleotides used for screening. The clones could be sorted into two categories, according to hybridization patterns of the single-stranded Bluescript form with sense and antisense oligonucleotides, to predict putative 5' and 3' orientations with respect to a presumed authentic clone encoding the gp90^{MEL-14} protein. The 5' orientations of the clones were identified, sequenced, and analyzed; we were then able to identify a single clone, of approximately 1550 bp, encoding, in the region hybridizing to the probe, a protein containing the sequence obtained by amino acid sequencing as well as all other predicted downstream amino acid residues (Fig. 1). The single possible exception was a tentative valine assignment at position 28; in that alanine was deduced to be at that position in the nucleotide sequence, this represented slightly out-of-step cleavage.

Transcript and genomic analysis of mLHR_c. RNA blot analysis was performed with selected polyadenylated RNA from both lymphoid cell lines and normal murine tissues (Fig. 2). The RNA blot was hybridized with a full-length mLHR_c insert. All cell lines and tissues expressing detectable mRNA, except testis, showed identical patterns with bands at 1.5, 2.5, and 5.2 kb. The intensity of hybridization correlates with cell surface expression of gp90^{MEL-14} (Fig. 3).

We have immuno-selected by cell-sorting a number of variants of EL-4, which differ with respect to surface expression of gp90^{MEL-14}. One group of variants derives from our original EL-4 cell line, characterized as low in antigen expression, from which the index EL-4-14hi was selected and stabilized (12). In addition, a transiently even higher expressing cell, designated EL-4-MEL-14Xhi, was selected. The patterns on RNA blot analysis corresponding to mRNA from EL-4-MEL-14Xhi, EL-4-MEL-14hi, and EL-4-MEL-14lo are shown (Fig. 2, as lanes A, B, and D, respectively). The transcript abundance parallels cell surface expression (Fig. 3A). Since there is a particular relative decrement in the amount of the 1.5-kb transcript species (Fig. 2, lane d) in the EL-4-MEL-14lo cells, this species may have a prominent role in determining cell surface expression. We also obtained an independent EL-4 clonal cell line (27) that demonstrated a distinct MEL-14 staining pattern containing two discrete populations of cells—a predominant negative population and a relatively small population, about 5 percent, of cells expressing gp90^{MEL-14}. Both the 3 percent brightest intensity and negative cells were sorted (Fig. 3B), immediately expanded, and mRNA extracted. Expression of the transcript in RNA blots is present in the high populations (Fig. 2, lane C) and absent in the negative population (Fig. 2, lane E), thereby showing, in combination with the variants described above, cosegregation of transcript and cell-surface antigen expression in variants derived from the same clonal cell-line.

Two other T cell lymphoma lines, VL-3 and C6VL, the former expressing relatively little surface antigen and the latter showing no cell surface staining, also show transcript patterns paralleling surface expression, with transcript present in VL-3 mRNA (Fig. 2, lane G), and absent in C6VL (Fig. 2, lane F). Also an *in vitro* B cell line, 38C13, expressing high surface levels of gp90^{MEL-14} also showed concordant abundance of the same transcripts. Therefore, qualitative and quantitative cell surface expression appears to parallel transcript abundance in these murine lymphoma cell lines.

Normal tissues show a predominant lymphoid distribution, paralleling tissue staining patterns for MEL-14 (Fig. 2, lanes H-N). Thymus, spleen, and mesenteric lymph node are positive for the 1.5-, 2.5-, and 5.2-kb transcripts found in cell lines, while liver, kidney, and brain show no detectable transcripts. Whereas the abundance of transcript in lymph node appears low, only about 2 μ g of this mRNA was available for analysis, thereby reducing its relative intensity. Testis is also devoid of any prominent bands, but appears to contain two smaller, diffuse, faintly hybridizing bands not shared by any of the bands in lymphoid cells or tissues (Fig. 2, lane M).

Genomic liver DNA from eight strains of mice were digested with Eco RI, Bam HI, and Xho I and subjected to DNA blot analysis; with subsequent hybridization to the full-length mLHR_c cDNA probe. A single identically sized hybridizing band with each enzyme was obtained in all strains tested. We conclude that under high stringency there is no evidence of polymorphism in this system.

Expression of MEL-14 determinants by mLHR_c. To establish that the clone isolated encodes a molecule bearing the MEL-14

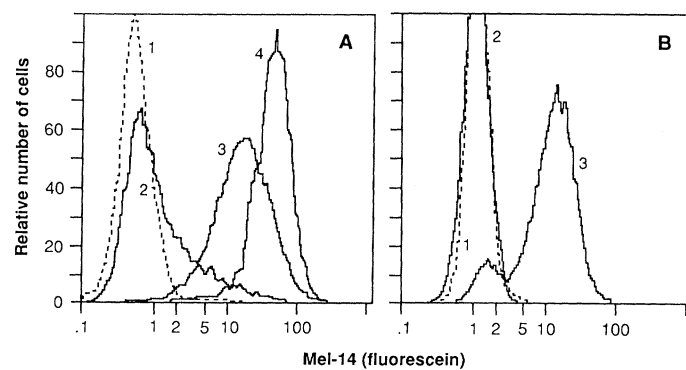


Fig. 3. Analysis (FACS) of cell lines varying with respect to expression of gp90^{MEL-14}. Cells were stained with an isotype matched control (A1, B1) or MEL-14 hybridoma supernatant (all others), and then treated with fluorescein isothiocyanate (FITC)-conjugated goat antibody to rat immunoglobulin adsorbed for cross reactivity with mouse serum components. (A) 1, EL-4-MEL-14hi; 2, EL-4-MEL-14; 3, EL-4-MEL-14hi; 4, EL-4-MEL-14Xhi. (B) 1, BD EL-4-MEL-14, positive sort; 2, BD EL-4-MEL-14lo, negative sort; 3, BD EL-4-MEL-14, positive sort.

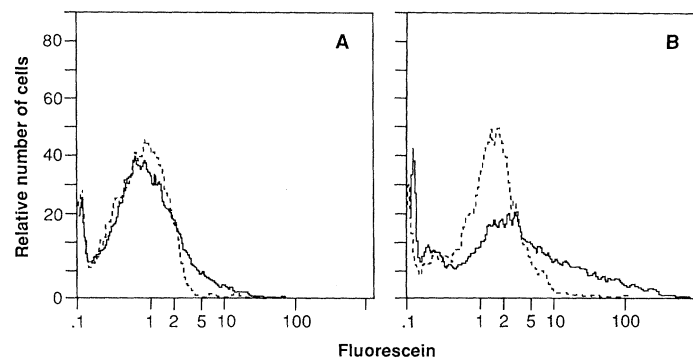
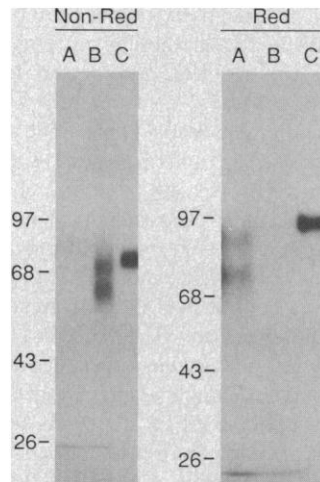


Fig. 4. FACS analysis of COS-7 cells transfected with mLHR_c DNA. The full-length cDNA clone was transferred to the expression vector CDM8 (67). Plasmid DNA was transfected into confluent COS-7 cells by the DEAE-dextran procedure (68). Enrichment of MEL-14 positive transfectants was achieved by plating transfected cells stained with MEL-14 onto petri dishes coated with goat antibody to rat Ig. Non-adherent cells were removed, and after 0.5 to 1 hour, adherent cells were removed, incubated at 37°C overnight, and again analyzed by fluorescence staining. (A) Dashed line, mLHR_c transfected COS-7 cells stained with isotype control; solid lines, same cells stained with MEL-14. (B) Dashed lines as in (A); solid lines, MEL-14 enriched positive transfectants, stained with MEL-14.

Fig. 5. Immunoprecipitation of MEL-14 reactive cell surface determinants from enriched mLHR_c transfected COS-7 cells. The mLHR_c transfected COS-7 cells, enriched as in Fig. 4, were surface-labeled with ¹²⁵I with lactoperoxidase. Immunoprecipitations and electrophoreses were performed as described (24) with the use of slab polyacrylamide gels under nonreducing and reducing conditions. Non-reducing gel: (lane A) transfectants, isotype control; (lane B) transfectants, MEL-14 antibody; (lane C) EL-4-MEL-14hi, MEL-14 antibody. Reducing gel: (lane A) transfectants, MEL-14 antibody; (lane B) transfectants, isotype control; (lane C) EL-4-MEL-14hi, MEL-14 antibody.



epitope, COS-7 cells were transfected with a vector containing the full-length mLHR_c, and cell surface expression was assessed by cytofluorometric analysis. Analysis of the transfected cells (Fig. 4A) shows a population of positive cells when stained with MEL-14 compared to staining with an isotype-matched control antibody. Identical backgrounds were obtained on staining mock transfected or Thy-1 transfected COS-7 cells with MEL-14. Integration analysis shows 6 percent of cells staining over background.

Transfections were enriched for cells bearing surface gp90^{MEL-14} for use in cell surface iodination and immunoprecipitation analyses (Fig. 4B). These selected cells were surface-labeled with ¹²⁵I and immunoprecipitated with MEL-14 (Fig. 5). Two MEL-14 specific species were present under nonreducing conditions, one slightly smaller than the mature gp90^{MEL-14} from EL-4-MEL-14hi (Fig. 5, lane B, non-reduced) at about 70 kD, and a smaller band of about 60 kD. This indicates probable processing of the transcript into discrete forms, and perhaps reflects alternative pathways of post

```

Met Val Phe Pro Trp Arg Cys Glu -31
CAG GTG GAG GAG CCT GAG GCC TGC AGA GAG ACT TGC AGA GAG ACC CAG CAA GCC ATG GTG TTT CCA TGG AGA TGT GAG 78

Gly Thr Tyr Trp Gly Ser Arg Asn Ile Leu Lys Leu Trp Val Trp Thr Leu Leu Cys Cys Asp Phe Leu Ile His His -5
GGT ACT TAC TGG GGC TCG AGG AAC ATC CTG AAG CTG TGG GTC TGG ACA CTG CTC TGT TGT GAC TTC CTG ATA CAC CAT 156
+1
Gly Thr His Cys Trp Thr Tyr His Tyr Ser Glu Lys Pro Met Asn Trp Glu Asn Ala Arg Lys Phe Cys Lys Gln Asn 22
GGA ACT CAC TGT TGG ACT TAC CAT TAT TCT GAA AAG CCC ATG AAC TGG GAA AAT GCT AGA AAG TTC TGC AAG CAA AAT 234
Tyr Thr Asp Leu Val Ala Ile Gln Asn Lys Arg Glu Ile Glu Tyr Leu Glu Asn Thr Leu Pro Lys Ser Pro Tyr Tyr 48
TAC ACA GAT TTA GTC GCC ATA CAA AAC AAG AGA GAA ATT GAG TAT TTA GAG AAT ACA TTG CCC AAA AGC CCT TAT TAC 312
Tyr Trp Ile Gly Ile Arg Lys Ile Gly Lys Met Trp Thr Trp Val Gly Thr Asn Lys Thr Leu Thr Lys Glu Ala Glu 74
TAC TGG ATA GGA ATC AGG AAA ATT GGG AAA ATG TGG ACA TGG GTG GGA ACC AAC AAA ACT CTC ACT AAA GAA GCA GAG 390
Asn Trp Gly Ala Gly Glu Pro Asn Asn Lys Lys Ser Lys Glu Asp Cys Val Glu Ile Tyr Ile Lys Arg Glu Arg Asp 100
AAC TGG GGT GCT GGG GAG CCC AAC AAC AAG AAG TCC AAG GAG GAC TGT GTG GAG ATC TAT ATC AAG AGG GAA CGA GAC 468
Ser Gly Lys Trp Asn Asp Asp Ala Cys His Lys Arg Lys Ala Ala Leu Cys Tyr Thr Ala Ser Cys Gln Pro Gly Ser 126
TCT GGG AAA TGG AAC GAT GAC GCC TGT CAC AAA CGA AAG GCA GCT CTC TGC TAC ACA GCC TCT TGC CAG CCA GGG TCT 546
Cys Asn Gly Arg Gly Glu Cys Val Glu Thr Ile Asn Asn His Thr Cys Ile Cys Asp Ala Gly Tyr Tyr Gly Pro Gln 152
TGC AAT GGC CGT GGA GAA TGT GTG GAA ACT ATC AAC AAT CAC ACG TGC ATC TGT GAT GCA GGG TAT TAC GGG CCC CAG 624
Cys Gln Tyr Val Val Gln Cys Glu Pro Leu Glu Ala Pro Glu Leu Gly Thr Met Asp Cys Ile His Pro Leu Gly Asn 178
TGT CAG TAT GTG GTC CAG TGT GAG CCT TTG GAG GCC CCT GAG TTG GGT ACC ATG GAC TGC ATC CAC CCC TTG GGA AAC 702
Phe Ser Phe Gln Ser Lys Cys Ala Phe Asn Cys Ser Glu Gly Arg Glu Leu Leu Gly Thr Ala Glu Thr Gln Cys Gly 204
TTC AGC TTC CAG TCC AAG TGT GCT TTC AAC TGT TCT GAG GGA AGA GAG CTA CTT GGG ACT GCA GAA ACA CAG TGT GGA 780
Ala Ser Gly Asn Trp Ser Ser Pro Glu Pro Ile Cys Gln Val Val Gln Cys Glu Pro Leu Glu Ala Pro Glu Leu Gly 230
GCA TCT GGA AAC TGG TCA TCT CCA GAG CCA ATC TGC CAA GTG GTC CAG TGT GAG CCT TTG GAG GCC CCT GAG TTG GGT 858
Thr Met Asp Cys Ile His Pro Leu Gly Asn Phe Ser Phe Gln Ser Lys Cys Ala Phe Asn Cys Ser Glu Gly Arg Glu 256
ACC ATG GAC TGC ATC CAC CCC TTG GGA AAC TTC AGC TTC CAG TCC AAG TGT GCT TTC AAC TGT TCT TCT GAG GGA AGA GAG 936
Leu Leu Gly Thr Ala Glu Thr Gln Cys Gly Ala Ser Gly Asn Trp Ser Ser Pro Glu Pro Ile Cys Gln Glu Thr Asn 282
CTA CTT GGG ACT GCA GAA ACA CAG TGT GGA GCA TCT GGA AAC TGG TCA TCT CCA GAG CCA ATC TGC CAA GAG ACA AAC 1014
Arg Ser Phe Ser Lys Ile Lys Glu Gly Asp Tyr Asn Pro Leu Phe Ile Pro Val Ala Val Met Val Thr Ala Phe Ser 308
AGA AGT TTC TCA AAG ATC AAA GAA GGT GAC TAC AAC CCC CTC TTC ATT CCT GTA GCC GTC ATG GTC ACC GCA TTC TCG 1092
Gly Leu Ala Phe Leu Ile Trp Leu Ala Arg Arg Leu Lys Lys Gly Lys Lys Ser Gln Glu Arg Met Asp Asp Pro Tyr 334
GGG CTG GCA TTT CTC ATT TGG CTG GCA AGG CGG TTA AAA AAA GGC AAG AAA TCT CAA GAA AGG ATG GAT GAT CCA TAC 1170

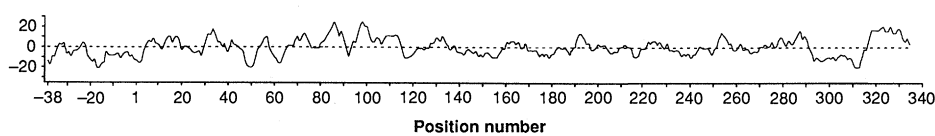
TGATTCATCCTTTGTGAAAGGAAAGCCATGAAGTGCTAAAGACAAAACATTGGAAAATAACGTCAGTCTCCCGTGAAGATTTTACACGCAGGCATCTCCCA 1273
CATTAGAGATGCAGTGTGCTCAACGAATCTGGAAGGATTTCTTCATGACCAACAGCTCCTCCTAATTTCCCTCGCTCATTTCATCCCATTAACCCATATCCC 1376
ATAATGTGTGCTCTATACAGAGTAGTATTTTATCATCTTTTCTGTGGAGGAACAAGCAAAAGTGTACTGTAGAATAAAGACAGCTGCTTTTACTCTTTCTCT 1479
AAAAAAAAAAAAAAAAAAAA 1497

```

Fig. 6. Complete nucleotide and predicted protein sequence of mLHR_c cDNA. The nucleotide sequence of the cDNA was determined by the dideoxy chain termination method (69), with the engineered T7 DNA polymerase Sequenase system (U.S. Biochemical Corp.). Single-stranded template DNA's were derived from either pBluescript SK(-) (excised from original λZAP isolates), Bluescript KS(-), or versions of bacteriophage M13mp18 and mp19. When sequences encoding the amino terminus predicted by amino acid sequencing of gp90^{MEL-14} were identified, appropriate restriction fragments were subcloned to derive internal sequence. Subsequently, oligonucleotide primers were synthesized to obtain remaining sequence of the full-length clone and to obtain second strand sequence where needed. The predicted protein sequence is indicated above the nucleotide

sequence beginning with the initiator methionine at nucleotide position 55; numbering to the right indicates the nucleotide and protein positions. Cysteine residues in the mature protein are marked with an asterisk (*) above, and canonical N-linked carbohydrate recognition sites (Asn-X-Ser or Thr) are overlined with arrow bars, as is the transmembrane region. The 15 nucleotides encoding the NH₂-terminal five amino acids and hybridizing to the oligonucleotide probe used for screening are underlined. Though a strictly conventional polyadenylation splice site AATAAA was not present, a possible variant was identified at position 1450, ATATAAA followed by a common polyadenylation site, CAGCT, from 1459 to 1463, and a consensus poly(A) site CT just preceding the poly(A) tail. Potential poly(A) splice and common polyadenylation recognition sequences are double underscored.

Fig. 7. Hydropathy plot of the protein predicted by the mLHR_c DNA sequence. Analysis was performed with Microgenie (Beckman Instruments) software, which computes hydrophobicity with the algorithm of Kyte and Doolittle (30). Regions above the dashed line indicate relative hydrophilicity, regions below the dashed line indicate relative hydrophobicity.



translational modification, including glycosylation and ubiquitination or both. The latter possibility is particularly intriguing since the difference in molecular mass between the bands is consistent for addition of a single ubiquitin moiety (8.5 kD). In fact, the non-glycosylated form of gp90^{MEL-14} is 45 kD (28); and here we demonstrate that mLHR_c encodes a 37-kD protein, also a single ubiquitin moiety size difference. While the sizes are slightly altered (Fig. 5) from the EL-4-MEL-14-hi form, the typical reducing and non-reducing behavior of gp90^{MEL-14} (that is, with non-reduced form migrating faster than reduced form) is retained.

The complete nucleotide sequence of the entire cDNA clone, determined on both strands, and its predicted protein sequence is shown in Fig. 6. The clone has a 54-bp 5' untranslated region followed by a single initiator ATG codon, which begins an uninterrupted open reading frame of 1116 bp. The TGA stop codon at position 1170 is followed by 327 bp of 3' untranslated region. The assignment of the initiator ATG is supported by the presence of flanking sequence falling within those typifying eukaryotic initiator sites, in this case GCCATGG (29).

The reading frame encodes a protein with a hydrophobic leader sequence 38 amino acids in length, before the initial tryptophan residue of the mature protein. The length of the leader sequence is unusual for a eukaryotic signal sequence. While hydropathy analysis (30) (Fig. 7) confirms a generally hydrophobic leader sequence, the initial 15 residues are neutral to slightly hydrophilic. The apparent signal sequence is also distinctive in that it is enriched in cysteine (four residues) and histidine (three residues), largely clustered in the 12 residues preceding the mature protein. The unusual features together suggest the possibility of specialized pathways of intracellular traffic.

The mature protein begins with a tryptophan, a highly unusual amino-terminal amino acid. It has ten potential asparagine-linked glycosylation sites, consistent with our protein characterization data showing extensive glycosylation on endoglycosidase F digestion (24), and subsequent tunicamycin experiments (28). Six of these are contained within the identical repeat unit structure. No clusters of Ser or Thr (or both), characteristic of sites of O-linked glycosylation, are present in the deduced sequence, an observation confirmatory of our inability to find evidence for O-linked glycosylation in cell surface and metabolic labeling studies of gp90^{MEL-14} (28). The mature protein contains 22 cysteine residues, comprising 6.6 percent. Twelve of the cysteines are present in the complement regulatory protein (CRP) repeat sequence, and nine other cysteines are concentrated in the 60 amino acid sequence just preceding the repeat units in the epidermal growth factor-like (EGF) domain, resulting in a highly cysteine-rich pre-transmembrane region of 180 to 190 amino acids.

The deduced mature protein is 334 amino acids long, with a calculated molecular size of 37 kD. A hydrophobic transmembrane region encompassing amino acids from about 295 to 317 is followed by a cluster of positively charged residues and a hydrophilic cytoplasmic tail of 18 amino acids. The hydropathy plot (Fig. 7) further shows distinct regions of relative hydrophilicity, concentrated in the NH₂-terminal 150 amino acids and in the membrane proximal approximate 20 amino acids. The intervening extracytoplasmic portion consists of a relatively uncharged neutral stretch that includes the EGF and CRP domains.

Carbohydrate-binding proteins are generally homologous to each other in a carboxyl-terminal domain of 130 to 150 residues, a region containing the carbohydrate-binding activity (31–33). The mLHR_c is homologous in particular to the hepatic lectins of human and rat (32, 34) over the NH₂-terminal 118 amino acids, and to virtually all animal lectins over a stretch of 45 amino acids (74 to 118) equivalent to the 50 COOH-terminal residues of the binding domain in animal lectins (Fig. 8A). This region includes three invariant cysteines at 90, 109, and 116 in mLHR_c, Asn-Trp at 75 and 76, a characteristic Glu-Pro-Asn (80 to 82), a Glu at 88, Cys-Val at 90 and 91, and the conserved Gly-X-Trp-Asn-Asp at 102 to 106. Only a highly conserved Gly¹² in the consensus sequence and present in other mammalian lectins, is absent from the presumed carbohydrate-binding domain in mLHR_c. Between conserved residues Asn⁸² and Glu⁸⁸ (the region where the conserved Gly is absent), there is a cluster of three lysine residues; and there is an insertion relative to the consensus sequence of seven amino acids, five of which are charged, between Cys¹⁷ and Gly²³ of the consensus sequence. No other insertions or deletions are required to align this portion of the mLHR_c sequence with the consensus sequence. This portion of the domain in mLHR_c contains ten positively charged residues, three Arg and seven Lys. Comparison to the analogous portion of carbohydrate-binding domains of other animal lectins show rat hepatic lectin-1 (RHL-1) to be the most enriched in basic amino acids with four arginines in the same region, and no lysines. Other mammalian lectins containing Lys in this region are the mannose-binding protein C (MBP-C) of rat and human, and human IgE (immunoglobulin E) Fc receptor, each of which has a single Lys, and canine pulmonary surfactant apoprotein with two lysines. The orientation of the lectin domain in mLHR_c is unusual, being inverted with respect to other animal lectins, which are oriented with the NH₂-terminus anchored in the plasma membrane and the COOH-terminus containing the binding portion extending extracellularly.

The presence of a lectin domain in gp90^{MEL-14} is entirely consistent with studies showing that mannose 6-phosphate and some analogues, but not other carbohydrates, inhibit binding to peripheral lymph node HEV, but not Peyer's patch (35). Also, MEL-14 has been shown to inhibit specifically the binding of lymphocytes to polystyrene beads derivatized with PPME (a polyphosphomonoester mannan fragment rich in mannose 6-phosphate), suggesting a close association of these determinants. Nevertheless, excess soluble PPME does not inhibit binding of MEL-14 to cells (36), so that identity of the MEL-14 and carbohydrate-binding determinants is unlikely. Since MEL-14 appears to recognize a ubiquitin-dependent determinant (24, 25), the preponderance of Lys in the region suggests possible candidate sites for ubiquitination. Particularly intriguing is this lysine-rich region of the lectin domain.

The EGF-like domain in mLHR_c consists of a single-copy homolog of the EGF repeat unit, which preserves many of the Cys or Gly residues characteristic of this structure (118 to 155) (Fig. 8B). All six consensus cysteines are present as well as Gly¹⁴⁷ and Gly¹⁵⁰, and Tyr¹⁴⁸ of mLHR_c. The relation (alignment) of these conserved residues is identical to that of human and bovine blood clotting factors IX and X, and the drosophila *notch* gene product (in all but 4 of 36 repeats in this gene), but not to the other molecules

receptor repeat structure to complement than to other proteins.

While homologous repeat units are not unusual among cell surface and other proteins, the presence of a precisely identical repeat unit from nucleotide positions 634 to 819 and 820 to 1006 is distinctive. Since cDNA library screening resulted in a single full-length clone to analyze, it was important to establish that this feature reflected the actual mRNA sequence rather than an artifact introduced during cloning. To ascertain the presence of the duplicated sequence in the actual mRNA, we performed a polymerization chain reaction (45) experiment. Using two oligonucleotide primers, one beginning at nucleotide 218 and the other ending at nucleotide 1434, we were able to predict an amplified fragment of 1217 bp (Fig. 6). Amplification was performed on isolated Bluescript SK(-) plasmid containing the full-length mLHR_c insert, EL-4/MEL-14hi mRNA derived cDNA, or control mRNA derived cDNA. The results (Fig. 9), demonstrate an identically sized major band from both the Bluescript clone and the newly synthesized EL-4/MEL-14hi cDNA (Fig. 9, lanes B and C), at the size consistent with a repeated subunit. As further confirmation of this interpretation, the amplified DNA from both the clone and EL-4-MEL-14hi cDNA were mapped with the restriction enzymes Pst I (Fig. 9, lanes E and F) and Kpn I (lanes G and H), both of which cut within the repeat unit structure. The digests show identical bands from both amplified DNA's. The band sizes predicted from the sequence in Fig. 6, 546 and 485 bp for Pst I, and 576 and 454 bp for Kpn I, are confirmed by the gel. These results affirm that the sequence of the clone analyzed represents the sequence in intact mRNA. In addition, if represented in the oligonucleotide-primed cDNA, it suggests that the other two larger transcripts contain the same sequence over this interval and that variation in these transcripts more likely resides in the 5' and 3' flanking portions of these species. The finding of an identical rather than homologous repeat of the CRP-like sequence is striking. This implies a very recent gene segment duplication, rather than a reduction to two units from a multi-unit ancestor segment by unequal crossing-over. It will be of interest to trace the evolutionary history of this unit and to compare homologous units, if present, in other mammalian homing receptors.

The mLHR_c sequence represents a tandem accumulation of

Fig. 9. Poly(A) selected EL-4-MEL-14hi RNA was primed with poly(dT) and converted into double-stranded cDNA. Two oligonucleotides were synthesized to permit amplification over the region of interest, one (19 nucleotides) hybridizing to the antisense strand of the cDNA 5' to the repeat unit, at positions 218 to 236, and the other (18m nucleotides) hybridizing to the sense strand in the 3' untranslated segment, from positions 1417 to 1434. The polymerase chain reaction was conducted with a Cetus-Perkin-Elmer PCR unit and Taq I polymerase. Ten percent of each resulting sample was subjected to electrophoresis on a 1.5 percent agarose gel directly or after digestion with a single restriction enzyme. (Lane A) Amplified C6V1 mRNA derived cDNA, negative control; (lanes B, E, and G) amplified mLHR_c DNA; (lanes C, F, and H) amplified EL-4-MEL-14hi mRNA derived cDNA; (lane D) amplified EL-4-MEL-14hi mRNA derived cDNA primed with Ly-6 specific oligos. Undigested (lanes B and C) Pst I digest, lanes E and F; Kpn I digest, lanes G and H. Size of mobility standards are indicated in kilobases.

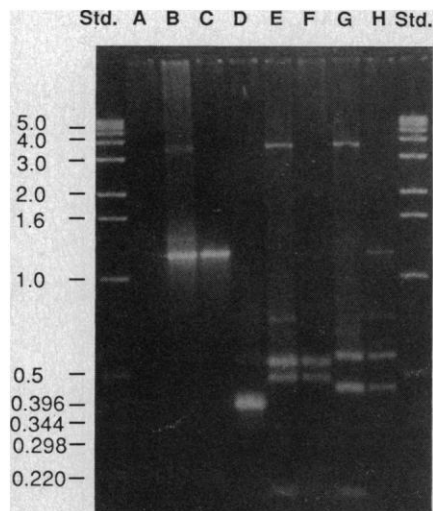


Fig. 10. Schematic representation of the mature mLHR_c protein structure. Lectin, lectin (carbohydrate binding) domain; EGF, epidermal growth factor-like domain; CRP_{1/2}, complement regulatory protein repeat domains; TM, transmembrane region.

diverse sequences (Fig. 10), all of which participate in intermolecular interactions, and which may be expressed at the cell surface. The targets of these interaction "domains" are either well-known (sugars or glycoproteins for the animal lectins (31-33), C3 or C4 (or both) fragments for complement regulatory proteins (46-48), and the c-erb-B product for EGF, or speculated on; that is, the enhancer of split product for *notch* (37, 49). The EGF-like repeat, in fact, finds homology not only in cell-surface developmental cell-interaction molecules such as the *notch* product and laminin b₁ (50), but also nematode *C. elegans lin-12* (51), and the LDL receptor (52), and is joined to a serine protease domain in a number of clotting factors (53). The primary known function of the mLHR is the migration of blood-borne lymphocytes to and through lymph node HEV's (54). The adhesive interaction between lymphocytes and HEV's is both highly specific and highly avid, as shown both by in vitro (4, 55) and in vivo (2, 56). After the initial binding event, the cells move through the HEV to the surrounding tissue extracellular matrix, and then T cells home to paracortex, while B cells home to primary follicles (11). The binding of lymphocytes to HEV is partially inhibited by antibodies to the LFA-1 member of the integrin family (38, 57), and completely inhibited by MEL-14 (12) or antibody to LPAM-1 (38). We propose that the avidity of the interaction and the successive events that follow HEV binding involve the recognition of HEV elements both by the tandem mLHR_c lectin-like, EGF-like, and CRP-like domains, and other accessory molecules such as LFA-1. The calcium dependence of lymphocyte-HEV interactions (4) and the site and function of ubiquitin attachment are still unclear. The mLHR_c sequence does not contain an aspartate-rich sequence common in calcium-binding proteins, although it is conceivable that the EGF-like sequence might be involved (58, 59). We must now begin to analyze not only the HEV carbohydrates involved in lymphocyte-HEV interactions (60), but also test whether these lymph node HEV express the c-erb-B gene or genes encoding or homologous to C3 or C4. Finally the mLHR molecule with its separate domains and ubiquitin binding site, as well as distinct transmembrane and cytoplasmic domains, is an ideal single chain polypeptide with which to study protein structure-function relations important in cell interactions and development.

REFERENCES AND NOTES

1. A. F. Pirro, *Quaderni di Anatomia Practica Ser. X N.1-2*, 86 (1954).
2. J. L. Gowans and E. J. Knight, *Philos. Trans. R. Soc. London Ser. B* **159**, 257 (1964).
3. V. T. Marchesi and J. L. Gowans, *ibid.*, p. 283.
4. H. B. Stamper, Jr., and J. J. Woodruff, *J. Exp. Med.* **144**, 828 (1976).
5. G. A. Gutman and I. L. Weissman, *Transplantation* **16**, 621 (1973).
6. J. C. Howard, S. V. Hunt, J. L. Gowans, *J. Exp. Med.* **135**, 200 (1972).
7. I. L. Weissman, *ibid.* **126**, 291 (1967).
8. ———, S. Baird, R. L. Gardner, V. E. Papaioannou, W. Raschke, *Cold Spring Harbor Symp. Quant. Biol.* **41**, 9 (1977).
9. G. A. Gutman and I. L. Weissman, *Adv. Exp. Med. Biol.* [Morphological and Functional aspects of immunity] **12**, 595 (1971).
10. ———, *Immunology* **23**, 465 (1972).
11. I. L. Weissman, G. A. Gutman, S. H. Friedberg, *Ser. Haematol.* **7**, 482 (1974).
12. W. M. Gallatin, I. L. Weissman, E. C. Butcher, *Nature* **304**, 30 (1983).
13. S. K. Stevens, I. L. Weissman, E. C. Butcher, *J. Immunol.* **128**, 844 (1982).
14. G. Kraal, I. L. Weissman, E. C. Butcher, *ibid.* **130**, 145 (1983).
15. J. C. Howard, S. V. Hunt, J. L. Gowans, *J. Exp. Med.* **135**, 200 (1972).
16. P. R. Streeter, E. L. Berg, B. T. Rouse, R. F. Bargatze, E. C. Butcher, *Nature* **331** **41** (1988).
17. R. F. Bargatze, N. W. Wu, I. L. Weissman, E. C. Butcher, *J. Exp. Med.* **166**, 1125 (1987).
18. B. T. Sher et al., *Adv. Cancer Res.* **51**, 361 (1988).

19. R. A. Rasmussen, Y. H. Chin, J. J. Woodruff, T. G. Easton, *Immunology* **135**, 19 (1985).
20. J. J. Woodruff and L. M. Clarke, *Annu. Rev. Immunol.* **5**, 201 (1987).
21. S. Jalkanen *et al.*, *Immunol. Rev.* **91**, 39 (1986).
22. S. Jalkanen, R. F. Bargatzke, J. de los Toyos, E. C. Butcher, *Cell Biol.* **105**, 983 (1987).
23. R. L. Idzorda *et al.*, *Proc. Natl. Acad. Sci. U.S.A.*, in press.
24. M. Siegelman *et al.*, *Science* **231**, 823 (1986).
25. T. St. John *et al.*, *ibid.*, p. 845.
26. Provided by D. Denney and J. Elliott.
27. Provided by Becton-Dickenson Immunocytometry Systems, Inc., Mt. View, CA.
28. M. van de Rijn, I. L. Weissman, M. H. Siegelman, in preparation.
29. M. Kozak, *RNA's*, *Nucl. Acids Res.* **12**, 857 (1984a); *Cell* **44**, 283 (1986).
30. J. Kyte and R. F. Doolittle, *J. Mol. Biol.* **157**, 105 (1982).
31. K. Drickamer, J. F. Mamon, G. Binns, J. O. Leung, *J. Biol. Chem.* **259**, 770 (1984).
32. M. Spiess and H. F. Lodish, *Proc. Natl. Acad. Sci. U.S.A.* **82**, 6465 (1985).
33. K. B. Chiacchia and K. Drickamer, *J. Biol. Chem.* **259**, 15440 (1984).
34. M. Spiess, A. L. Schwartz, H. F. Lodish, *ibid.* **260**, 1979 (1985); E. C. Holland, J. O. Leung, K. Drickamer, *Proc. Nat. Acad. Sci. U.S.A.* **81**, 7338 (1984).
35. L. M. Stoolman and S. D. Rosen, *J. Cell Biol.* **96**, 722 (1983); L. M. Stoolman, T. S. Tenforde, S. D. Rosen, *ibid.* **99**, 1535 (1984); T. A. Yednock, L. M. Stoolman, S. D. Rosen, *ibid.* **104**, 713 (1987).
36. T. A. Yednock, E. C. Butcher, L. M. Stoolman, S. D. Rosen, *J. Cell Biol.* **104**, 725 (1987).
37. K. A. Wharton, K. M. Johansen, T. Xu, S. Artavanis-Tsakonas, *Cell* **43**, 567 (1985); S. Kidd, M. R. Kelley, M. W. Young, *Mol. Cell Biol.* **6**, 3094 (1986).
38. B. Holzmann, B. W. McIntyre, I. L. Weissman, *Cell*, in press; B. Holzmann and I. L. Weissman, in preparation.
39. T. Kristensen and B. F. Tack, *Proc. Natl. Acad. Sci. U.S.A.* **11**, 3963 (1983).
40. D. J. Lipman and W. R. Pearson, *Science* **227**, 1435 (1985).
41. K. B. M. Reid *et al.*, *Immunol. Today* **7**, 230 (1986).
42. W. J. Leonard *et al.*, *Science* **230**, 633 (1985); N. Ishida *et al.*, *Nucleic Acids Res.* **13**, 7579 (1985).
43. J. Lozier, N. Takahashi, F. W. Putnam, *Proc. Natl. Acad. Sci. U.S.A.* **81**, 3640 (1984).
44. A. Ichinose, B. A. McMullen, K. Fujikawa, E. W. Davie, *Biochemistry* **25**, 4633 (1986).
45. K. Mullis *et al.*, *Cold Spring Harbour Symp. on Quant. Biol.* **51 Pt. 1**, 263 (1986); R. K. Saiki, T. L. Bugawan, G. T. Horn, K. B. Mullis, H. A. Erlich, *Nature* **324** (6093), 163 (1986).
46. T. Kinoshita and V. Nussenzweig, *J. Immunol. Methods* **71**, 247 (1984).
47. T. Kaidoh, T. Fujita, Y. Takata, S. Natsumme-Sakai, M. Takahashi, *Complement* **1**, 44 (1984).
48. S. Natsumme-Sakai, K. Sudoh, T. Kaidoh, J.-I. Hayakawa, M. Takahashi, *Immunol.* **134**, 2600 (1985).
49. W. J. Welshons, *Drosophila Inform. Surv.* **30**, 157 (1956).
50. D. J. Montell and C. S. Goodman, *Cell* **53**(3), 463 (1988).
51. I. Greenwald, *ibid.* **43**, 583 (1985); J. Yochem, K. Weston, I. Greenwald, *Nature* **335**, 547 (1988).
52. D. W. Russell, W. J. Schneider, T. Yamamoto, K. L. Luskey, M. S. Brown, J. L. Goldstein, *Cell* **37**, 577 (1984).
53. M. R. Fung, C. W. Hay, R. T. MacGillivray, *Proc. Natl. Acad. Sci. U.S.A.* **82**, 3591 (1985).
54. M. Gallatin *et al.*, *Cell* **44**, 673 (1986).
55. E. C. Butcher and I. L. Weissman, *Ciba Foundation Symp.* **71**, 265 (1980).
56. M. Bjercknes, H. Cheng, C. A. Ortaway, *Science* **231**, 402 (1986).
57. A. Hamann *et al.*, *J. Immunol.* **140**, 693 (1988).
58. B. A. McMullen *et al.*, *Biochemistry* **22**, 2875 (1983).
59. N. L. Esmon, L. E. DeBault, C. T. Esmon, *J. Biol. Chem.* **258**, 5548 (1983).
60. L. M. Stoolman, T. A. Yednock, S. D. Rosen, *Blood* **70**, 1842 (1987).
61. R. M. Hewick, M. W. Hunkapiller, L. E. Hood, W. J. Dreyer, *J. Biol. Chem.* **256**, 7990 (1981).
62. S. L. Beaucage and M. H. Curuthers, *Tetrahedron Lett.* **22**, 1859 (1981).
63. *Applied Biosystems User Bull.* **13**, 20 (1984).
64. T. Maniatis, E. F. Fritsch, J. Sambrook, *Molecular Cloning. A Laboratory Manual* (Cold Spring Harbor Laboratory, Cold Spring Harbor, NY, 1982).
65. H. Lehrach, D. Diamond, J. M. Wozney, H. Boedtker, *Biochemistry* **16**, 4743 (1977).
66. A. P. Feinberg and B. Vogelstein, *Anal. Biochem.* **132**, 6 (1983).
67. Provided by B. Seed.
68. A. Aruffo and B. Seed, *Proc. Natl. Acad. Sci. U.S.A.* **84**, 8573 (1987); B. Seed and A. Aruffo, *ibid.*, p. 3365.
69. F. Sanger, S. Nicklen, A. R. Coulson, *ibid.* **74**, 5463 (1977).
70. Supported by USPHS grant AI09022, NIH award OIG43551 (I.L.W.), a grant from the Weingart Foundation, Bristol-Myers Cancer Research fellowship (M.H.S.); a Multiple Sclerosis Society fellowship (M.v.d.R.). We thank D. Denney, J. Elliott, C. Okada, and P. Estess for support, ongoing discussion, and generosity with reagents; L. Jerabek for cell-sorting assistance; M. Bond, DNAX for amino acid sequencing; B. Summey and associates for execution of the graphics, and M. Finney for help in preparation of the manuscript.

30 December 1988; accepted 30 January 1989

